

Remote chemical, biological and explosive agent detection using a robot-based Raman detector

Charles W. Gardner^{*a}, Rachel Wentworth^a, Patrick J. Treado^a, Parag Batavia^b, Gary Gilbert^c

^aChemImage Corporation, 7301 Penn Ave., Pittsburgh, PA 15208;

^bApplied Perception, Inc., 220 Executive Drive, Cranberry Township, PA 16066

^cUS Army Telemedicine and Advanced Technology Research Center (TATRC), 504 Scott Street, Fort Detrick, MD 21702-5014

ABSTRACT

Current practice for the detection of chemical, biological and explosive (CBE) agent contamination on environmental surfaces requires a human to don protective gear, manually take a sample and then package it for subsequent laboratory analysis. Ground robotics now provides an operator-safe way to make these critical measurements. We describe the development of a robot-deployed surface detection system for CBE agents that does not require the use of antibodies or DNA primers. The detector is based on Raman spectroscopy, a reagentless technique that has the ability to simultaneously identify multiple chemical and biological hazards. Preliminary testing showed the ability to identify CBE simulants in 10 minutes or less. In an operator-blind study, this detector was able to correctly identify the presence of trace explosive on weathered automobile body panels. This detector was successfully integrated on a highly agile robot platform capable of both high speed and rough terrain operation. The detector is mounted to the end of five-axis arm that allows precise interrogation of the environmental surfaces. The robot, arm and Raman detector are JAUS compliant, and are controlled via a radio link from a single operator control unit. Results from the integration testing and from limited field trials are presented.

Keywords: robot, biowarfare, detector, Raman, spectroscopy, UGV, chemical warfare, explosives, JAUS

1. INTRODUCTION

This paper describes the feasibility demonstration of a chemical, biological and explosive (CBE) detection system based on Raman spectroscopic measurements integrated to a commercially available unmanned ground vehicle (UGV) platform. Raman detection offers potential advantages over immunoassay and DNA-based biological detection strategies using reagents, especially when configured for use on an unmanned vehicle. Raman measurements are reagentless, greatly simplifying the logistics of deployment. In addition, Raman measurements can be used to detect a broad range of CBE threats in a single measurement cycle. No assumption of the possible threat is required as in the case of reagent-based detection schemes.

By remotely guiding this sensor system to an incident area to assess soil, water and surface contamination, exposure of personnel to a hazardous environment is prevented until the nature of the threat is fully known. Bringing the sensor to the sample also minimizes problems associated with sampling, such as cross-contamination and pre-analysis decontamination as well as the problems of disposal after the analysis is complete.

1.1 Raman spectroscopy for CBE detection

Raman spectroscopy has been studied and used as a laboratory tool in chemistry for many years¹. It is now reaching a level of maturity that is transitioning from the laboratory to a variety of field applications. The Raman effect occurs when a photon encounters a molecule, during which time there is a chance that the energy from the scattered photon will be exchanged with vibrational bond energy of the molecule. This energy exchange manifests itself as a shift in frequency (or wavelength) in a small amount of the scattered light. Because each different chemical bond in a material causes a different frequency shift, the pattern of these shifts, known as the Raman spectrum, is unique to that material.

*cgardner@chemimage.com; phone 1 412 241 7335; fax 1 412 241 7311; chemimage.com

The Raman spectrum reveals the molecular composition of materials, including the specific functional groups present in organic and inorganic molecules. The Raman spectrum is a characteristic property of a material just like its color or melting point and can be used to determine the presence or absence of the material.

Several groups have shown the applicability of Raman spectroscopy to the detection of CBE agents. In a parallel program, ChemImage has been working to build the Raman Chemical Imaging for Biothreat Detection (RCIBD) library² in collaboration with the US Armed Forces of Pathology (AFIP). Currently, this library contains entries from over 1000 chemical, biological and explosive threat materials as well as many materials naturally present in environmental samples.

As an example of the applicability of Raman measurements, Figure 1 shows the Raman spectra from several nerve and blister chemical warfare agents³.

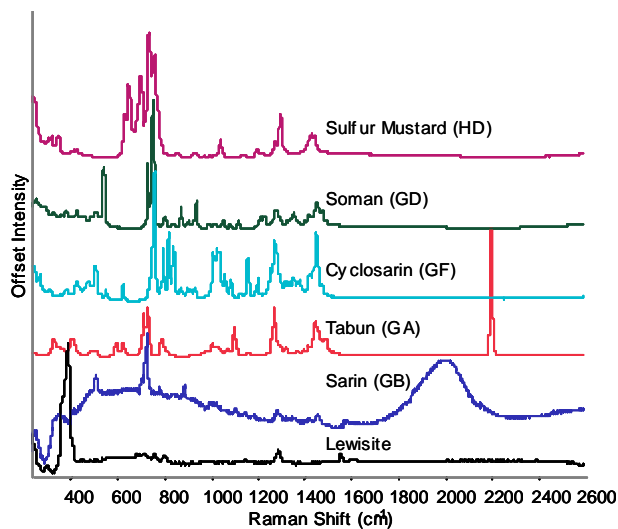


Fig. 1. Raman spectra of several chemical warfare agents

Figure 2 shows Raman spectra of several biological organisms that have been considered in biological warfare. Also included is the Raman spectrum of a known biological toxin, Ricin⁴.

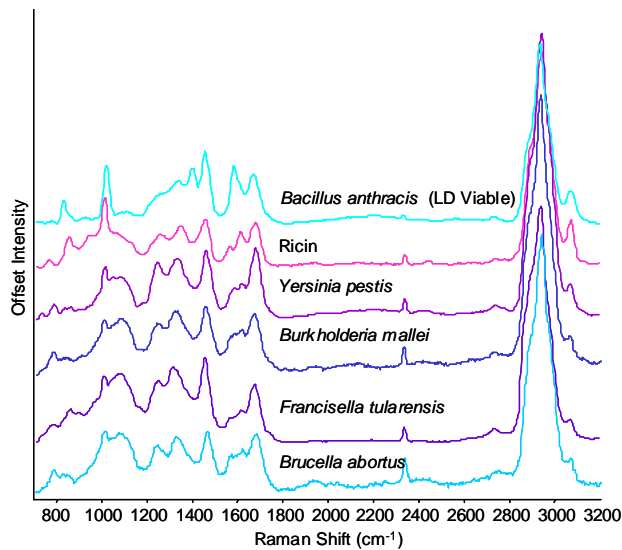


Fig. 2. Raman spectra of selected biothreat agents

Figure 3 shows the Raman spectra of some typical explosive materials. These were taken at ChemImage on a commercially available laboratory Raman system as a part of this study.

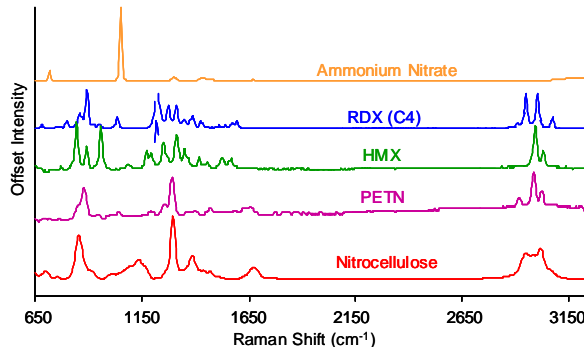


Fig. 3. Raman spectra of typical explosive materials.
RDX-Cyclotrimethylenetrinitramine
HMX-Cyclotetramethylene-tetranitramine
PETN - Pentaerythritol tetranitrate

These fundamental studies clearly demonstrate the potential for identification of CBE agents by Raman spectroscopy. However, reliable detection of CBE agents under actual environmental conditions will require more than just the ability to generate unique spectra.

The goal of this detector system is to identify CBE agents on environmental surfaces. Therefore, the detector will always be measuring an agent spectrum in the presence of the spectrum from the background or from any other material that may be present. Fortunately, in most real-world situations, the ratio of the amount of agent to the background and any other materials has significant spatial variation. This variation in composition leads to slightly different Raman spectra from different areas on the sample surface. These differences in spectra provide enough information for chemometric processing of the data, allowing identification of the agent and the background materials⁵.

Therefore, the CBE detector planned for UGV integration in this study will rely on both the inherent specificity of Raman measurements and on the improvement in identification reliability inherent in spatially resolved spectroscopic measurements.

2. METHODOLOGY

2.1 Raman detector

The Raman detector built in this study consists of a detector head mounted in the gripper of a UGV manipulator arm and an instrument package mounted on the UGV chassis. Since previous studies had shown that the optimum laser excitation wavelength for Raman biothreat detection was 532 nm, this system used a 100 mW 532 nm laser (B&W Tek) mounted in the instrument package and coupled into a 200 μm core diameter optical fiber, 4 m in length. The laser fiber terminated in the detector head where the light was collimated using a 18 mm focal length achromat lens doublet, filtered using a 532 nm bandpass filter (Semrock, Inc.) and directed to a 45° dichroic mirror (532 nm, Semrock, Inc.). The dichroic mirror reflected the laser light to a 8 mm focal length aspheric objective lens (numerical aperture (NA) of 0.5), which focused the laser on the sample. Centering of the laser on the objective lens was facilitated by a 2 degree-of-freedom (DOF) fiber mount and 5 DOF adjustment of the incoming laser beam position.

The laser stimulates both Rayleigh scattering (at the laser wavelength) and Raman scattering (wavelength shifted). A large fraction of the scattered light is collected by the objective lens and directed back towards the dichroic mirror. The dichroic mirror reflects most of the Rayleigh scattered light and allows the Raman scattered light at wavelengths longer than the laser wavelength to pass through. A sharp-edge, long pass filter (532 nm, Semrock) further reduces the amount of Rayleigh scattered light before a 27 mm focal length achromat lens focus the Raman light onto a bundle of 50 μm core diameter optical fibers, again, 4 m in length. At the other end of the fiber, the 19 fibers are translated into a linear array and placed at the input focal plane of a spectrograph with a 2 dimensional detector (Discovery, Headwall Photonics). The detector has a 122 x 1024 pixel format, which allows acquisition of an image containing the intensity

versus wavenumber data for each fiber. This image is transmitted over an Ethernet link to the system computer for further processing.

Targeting of the detector was facilitated using 2 video cameras mounted on the head. The first is a miniature color CMOS camera mounted as close as possible to the objective lens and focused at the focal plane of the Raman detector. The second is miniature video camera with pinhole lens, mounted to the outside of the detector case. This camera has a relatively large depth of focus so it is useful for viewing the area to be tested from a distance up to 2 m. In addition, a rubber camera lens hood is fixed to the optics end of the detector in order to block out ambient light during a measurement.

The system computer is a mini-ITX motherboard with 1 Gbyte of on-board memory, 4 USB ports and 2 Ethernet ports (CX 700, MSI). Additional peripherals for this system include a USB multifunction data acquisition module (Labjack U12) that controls the laser output and the safety shutter and a integrated stepper motor/controller (IMS) that controls the fine positioning of the detector head once it is mounted in the manipulator of the UGV. This computer used the CI Xpert software system (ChemImage Corp.) to control system components and for data collection and processing. The second Ethernet port is used for communication with a second single board computer (SBC) that serves to translate commands from the UGV computer operating in the joint architecture for unmanned systems (JAUS) environment to the detector SBC.

2.2 Unmanned ground vehicle (UGV)

The UGV chosen for the integration testing was the ARES (Applied Perception). This UGV is built on the RMP 400 Mobility Platform (Segway) and provides a JAUS compliant environment for up to two payload modules. For these tests, the ARES is controlled through an 802.11 wireless link from the operator control unit (OCU) based on a Toughbook CF-19 rugged laptop computer (Panasonic) and a wireless game controller (Logitech). The ARES also incorporates a wireless video link with 5 multiplexed inputs: 3 from the ARES chassis and 1 from each of the payload modules. The ARES also provides each payload module with 12 and 72 VDC and an Ethernet link into the UGV internal network.

The Raman detector system was designed to be easily integrated on the ARES and on several other small UGV systems. In order to position the Raman detector, the ARES was fitted with 5-DOF manipulator arm system (Oceaneering) controlled as one of the payload modules through a JAUS-compliant interface. The detector head is designed to fit within the gripper jaws of this arm and the electrical and optical cables are routed along the superstructure of the arm. The instrument package of the detector is mounted on a 15.275" x 18" x 0.5" (width x length x thickness) aluminum plate to facilitate easy installation and removal of the instrument package. Figure 4 shows the detector mounted on the ARES UGV as prepared for the integration testing.



Fig. 4. Raman detector integrated on the ARES UGV

2.3 Operator-blind explosive detection test

The substrate for the samples used in this test was circular sections of painted body panels from a scrapped Volkswagen Jetta (metallic green paint). The test samples were applied by either rubbing the test material into the surface (Arizona road dust and RDX explosive) or by spray (WD-40 oil). The detector was trained on a blank panel, as well as panels with oil, dust and RDX applied as the neat material and identified by the test monitor at the Army Research Laboratory (ARL). The detector was then presented with 6 test panels without any information as to their composition. The spectral data was collected from each of these samples and the identification was done off line.

3. RESULTS

3.1 Detector Performance

After the Raman sensor was assembled and aligned and prior to integration, its performance on several test samples was measured in the laboratory. Figure 5 shows the average detector response (blue trace) to a toxin stimulant, albumin (ovalbumin, Sigma-Aldrich) compared to a reference spectrum of the same material collected on a research-grade Raman microscope system (FALCON II, ChemImage). The similarity between the two spectra shows that the performance of the Raman sensor should be acceptable for the detection of other biothreat materials.

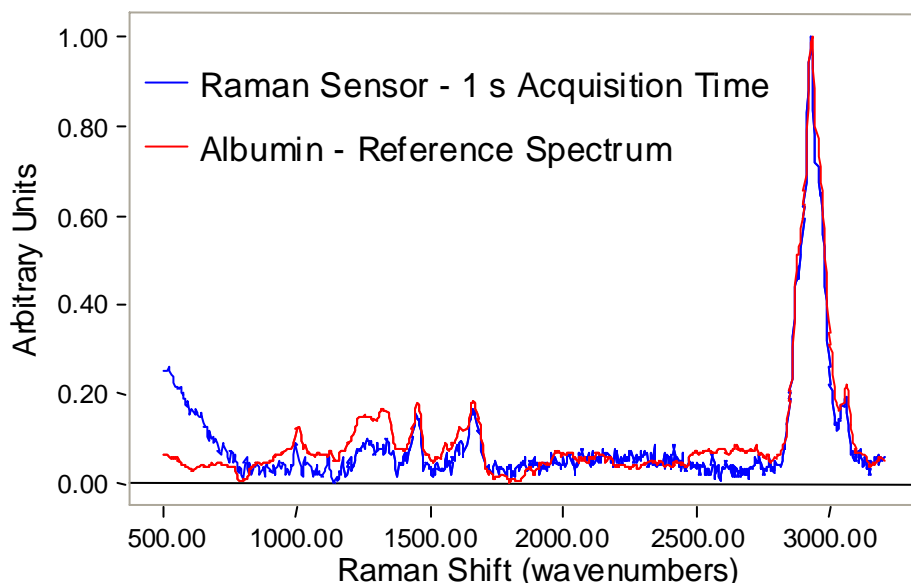


Fig. 5. Raman detector response to the toxin stimulant, albumin

While Figure 5 shows a single spectral trace, the Raman detector is actually producing a set of multiple spatially independent spectra from a single image from the spectrometer camera. This is done by applying a pixel map to the image that defines the detector rows corresponding to each fiber. The system software measures the intensity versus wavelength for each of the multiple fibers and stores these in a format that can be processed immediately or at a later time. Figure 6 shows both the camera image (spectral image) and the extracted spectra for a sample of acetaminophen.

A number of corrections are applied to the acquired spectra. Dark current correction divides the acquired spectra by a spectrum taken with the laser turned off. Instrument response is removed by correction with the NIST SRM 2242 Raman Intensity standard. This compares a spectrum taken of the NIST standard to the standard NIST spectra provided with the SRM. The difference is the instrument response, which is divided from the acquired spectra. Baseline fit is used to remove a sloped or curved baseline by finding the best least-squares baseline fit and subtracting it from each spectrum. Finally, the spectra are normalized to bring them all to the same intensity scale. The spectra are now ready to be used as the target in a spectral search.

There are a variety of algorithms that have been used to identify the components of a mixture. The first algorithm used in this work was a target-testing factor analysis based algorithm. To summarize, a set of mixture spectra is collected and is used to describe a mixture space using principal components analysis (PCA). Each library spectrum is then mapped into this space as a vector. If the mixture space completely describes all information about a given library spectrum, its angle of projection into the mixture space will be 0 (or a very small angle if there is noise in the set of mixture spectra). The library spectra can be ranked based on their angles and the top n matches are determined to be the pure components in the mixture, where n is the rank of the matrix associated with the mixture spectra. The angle of projection can also be used to determine if a given compound is a close enough match to be considered as a member of the mixture.

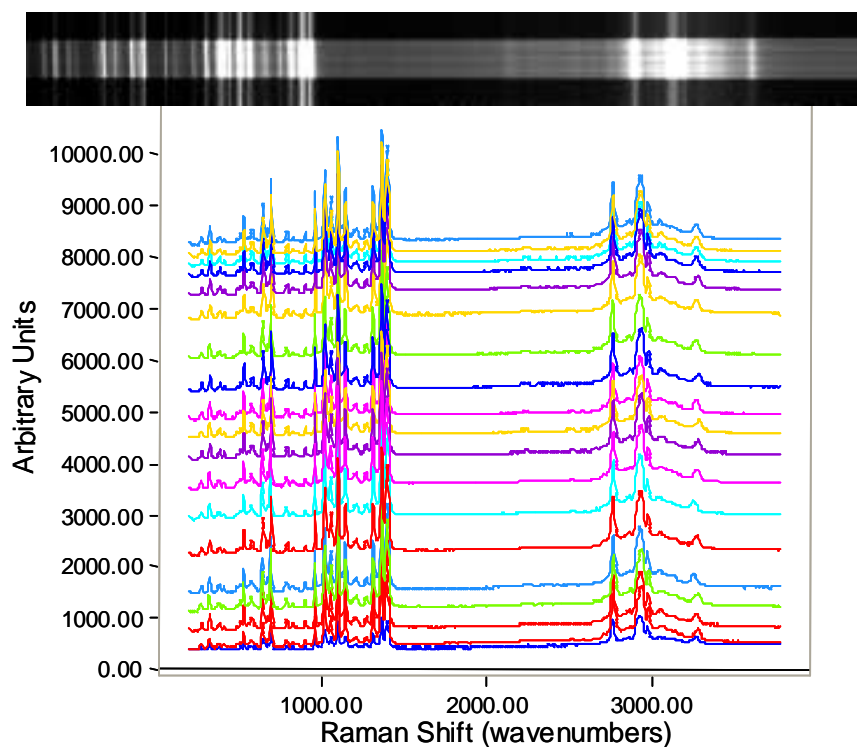


Fig. 6. Spectral image and multi-fiber spectra of acetaminophen taken with the Raman detector

The details of the implementation are as follows. The data set of multiple spectra is acquired and processed as described above. The spectra are then submitted to the spectral searching routine. The routine mathematically analyzes the set of spectra to determine if there is sufficient variability to indicate a mixture. If there is not sufficient variability, a mean spectrum is calculated from the multiple spectra and a simple Euclidean distance comparison is performed between the mean spectrum and each library spectrum. If there is sufficient variability, the set of multiple spectra is then submitted to the spectral unmixing algorithm as described above. In both cases, a score (Euclidean distance or target testing angle) is calculated for each entry in the library. A cutoff value for the score is used to determine if a library entry should be considered as the identified substance (either pure or as a member of a mixture). The classification of each identified substance (threat vs. non-threat) determines whether the physical substance under analysis can also be identified as a threat or non-threat.

ChemImage has also implemented a Mahalanobis distance classifier that depends on a class of spectra to identify pure substances rather than on a single spectrum. This algorithm was used instead of the Euclidean distance classifier in the explosives detection test.

Once searching is complete, the results are transmitted back from the RBI system computer to the operator control unit (OCU). Those library entries that are greater than the established cutoff are returned to the OCU as a text string for the name, followed by the confidence level.

3.2 Detector – UGV Integration

Once the Raman sensor performance was verified, the integration testing was started. The first set of tests was to verify the communications (UDP) between the detector SBC and the translator SBC over the Ethernet connection. Early in the development of the detector, a set of detector commands was developed that would be adequate to control and collect data from essentially any spectroscopic sensor. The next step was to write the translator software so that each detector command could be translated to or from a JAUS message. An area of particular concern was the transmission of the spectrum from the detector to the translator due to the relatively large size of the data packet (1024 x 16 bits at a minimum).

Once the translator was written and tested, the OCU was developed. The OCU controls the detector, the manipulator arm and the UGV chassis through a wireless link into the internal network of the UGV. The OCU developed in this study provides a basic interface for controlling the UGV through a wireless game controller but also provides specific screens for the status of the UGV chassis, the manipulator arm and the Raman detector. Each of these is easily selected from the OCU and switching between screens is straightforward.

Once the implementation of the JAUS messages was confirmed, the next step was the mechanical and electrical integration of the Raman detector on the ARES was tested. The detector head was positioned in the gripper of the manipulator arm and the electrical and optical cable bundle was attached to the arm using plastic wire ties. Care was taken to ensure that the cable bundle had enough slack to allow for the full range of movement of each of the manipulator joints. The instrument package was mounted to an ARES payload plate and placed in the rear payload position (the manipulator occupies the front payload position). The power, Ethernet and video connections were made between the instrument package and the ARES.

Early in testing it became evident that the ARES payload electrical power system could not support both the manipulator and the Raman detector simultaneously. It was therefore decided to power the laser from an auxiliary 10 Ah sealed lead acid battery, mounted on the payload plate, next to the detector. This solution solved the simultaneous operation problem between the arm and the detector and resulted in minimal system modification.

Once this problem was corrected, the communications and video subsystem integration was tested. Performance of both of these was acceptable and it was then able to demonstrate the operation of the complete UGV-based Raman detector system.

3.3 Operator-blind explosive detection test

Upon arrival in the ARL laboratory, the Raman detector was set up on the bench top, powered with a DC power supply and calibrated. The test monitor then gave the operator the training set disks. A multi-point spectral set was collected for each sample type, RDX, oil and the Arizona road dust as well as the spectral set corresponding to the blank panel. The operator was then presented with 6 test disks labeled A through F and a spectral data set collected from each of these using the same conditions as the training set.

The first step in the analysis was to extract the individual spectra from the camera image and correct for instrument response and dark current. Figure 7 shows the mean spectra from these data sets for the training set and for the unknown samples. At that point, the following subjective observations were made: First, the car panel (blank) and dust exhibit highest degree of spectral similarity. Second, the RDX sample provided a readily detectable explosive signature. Third, the unknown sample spectra were dominated by an unknown background interference. Despite this interference, the presence of RDX was evident in Samples D & E.

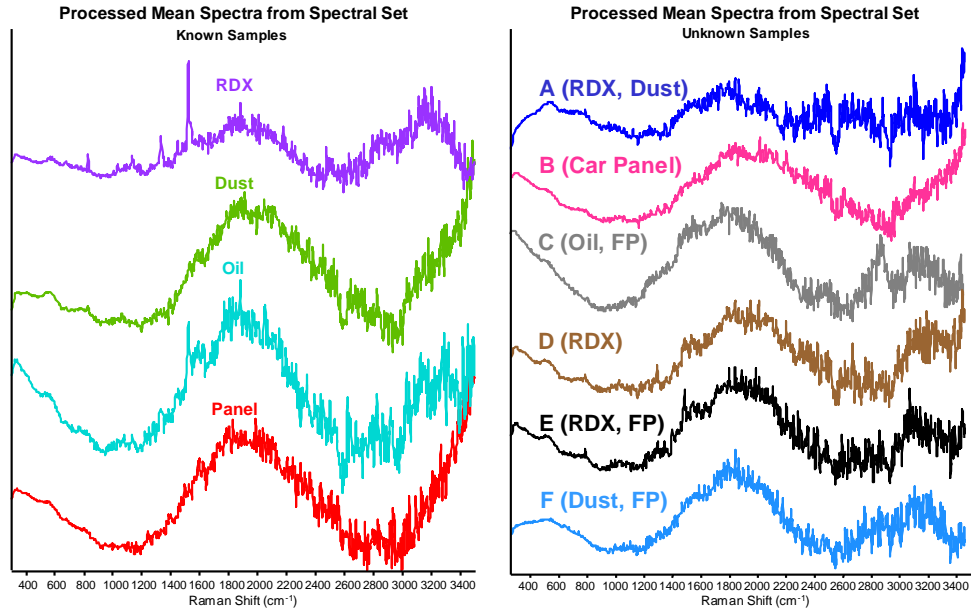


Fig. 7. Mean spectra from the multi-fiber spectral data set

The corrected spectral data sets were then analyzed as described in Section 3.1 using the Mahalanobis distance based classifier. Figure 8 shows the PCA plot of the data sets and indicates the variability inherent in the data. However, it was still possible to make the presumptive identifications shown in Table 1.

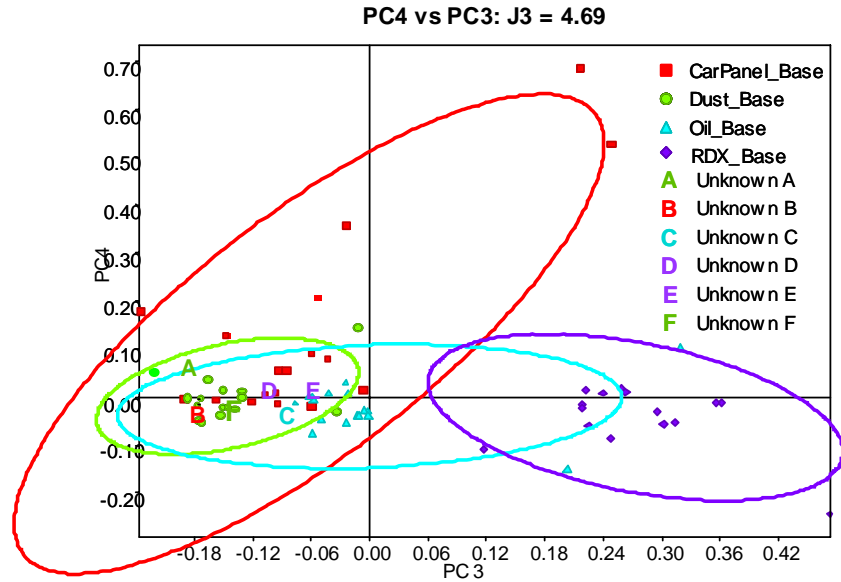


Fig. 8. Principal components analysis (PCA) plot for the training set and the test samples

Table 1. Final explosives detection test results

Unknown	Presumptive Identification	Actual Composition
A	Dust	RDX + Dust
B	Car Panel	Car Panel
C	Oil	Oil Fingerprints
D	RDX	RDX
E	RDX	RDX Fingerprints
F	Dust	Dust Fingerprints
Key to Test Results		
Correct ID	Partially Correct ID	Incorrect ID

The Raman detector made the correct identification of the sample composition in all case except for sample A. While the data analysis algorithms can identify the components of mixtures, the test monitors gave no indication that a mixture would be present, so the data analysis was not trained to look for mixtures. Therefore, we believe that the detector and the data processing were responding the component in the highest concentration, the road dust.

In order to “score” the performance of the Raman detector, the detection statistics shown in Table 2 were calculated from the results. While the specificity of the Raman detector in this test was excellent, we believe that the low sensitivity to RDX is due to the problems inherent with targeting particles of RDX on the car panel in the presence of dust and other materials.

Table 2. Detector performance in the operator-blind explosives test

	RDX	Dust	Car Panel	Oil
# of spectra tested	6	6	6	6
# True Positives (a)	2	2	1	1
# False Positives (b)	0	0	0	0
# False Negatives (c)	1	0	0	0
# True Negatives (d)	23	24	24	24
Sensitivity (a/(a+c))	66.67%	100%	100%	100%
Specificity (d/(b+d))	100%	100%	100%	100%
False Negative Rate (c/(a+c))	33.33%	0%	0%	0%
False Positive Rate (b/(b+d))	0%	0%	0%	0%
Positive Predictive (a/(a+b))	100%	100%	100%	100%
Negative Predictive (d/(c+d))	95.83%	100%	100%	100%

4. CONCLUSIONS

The feasibility of a Raman detector integrated in a JAUS-compliant UGV for use in the remote detection and identification of CBE agents in military and homeland security situations was demonstrated. This study showed detector-UGV integration, preliminary results with a biological agent (toxin) simulant and the results of an operator blind trial to detect explosives on car panels.

It also showed that a Raman sensor designed for the detection of biothreat agents could also be extended to the detection of RDX explosive on surfaces.

ACKNOWLEDGEMENTS

The authors would like to acknowledge the assistance of Dr. Andrzej Miziolek and his group at the Army Research Laboratory at Aberdeen Proving Ground for setting up and administering the operator-blind explosives detection test. Thanks go out to Scott Anderson, Robert Stern, and Jingyun Zhang from ChemImage for their work on the design and fabrication of the detector system. Thanks also to David Hsu from Applied Perception for his work on the JAUS translator interface.

We also thank Dr. Kathryn Kalasinsky of the Armed Forces Institute of Pathology for the biothreat agent Raman spectra and Dr. Steven Christesen of the Edgewood Chemical and Biological Center for the chemical warfare agent Raman spectra presented in this paper.

This work was supported by the US Army Medical Research and Materiel Command under Contract No. W81XWH-06-C-0010. The views, opinions and/or findings contained in this manuscript are those of the authors and should not be construed as an official Department of the Army position, policy or decision unless so designated by other documentation.

REFERENCES

- [1] Adar, F., Delhaye, M. and DaSilva, E. 2007: "Evolution of Instrumentation for Detection of the Raman Effect as Driven by Available Technologies and by Developing Applications", *J. Chem. Ed.*, 84(1), 50-60, (2007).
- [2] Kalasinsky, K., Hadfield, T., Shea, A., Kalasinsky, V., Nelson, M. P., Drauch, A. J., Powers, T., Vanni, G. S. and Treado, P. J., "Raman Chemical Imaging Spectroscopy (RCIS) Reagentless Detection and Identification of Pathogens: Signature Development and Evaluation". *Anal. Chem.*, 79(7), 2658 -2673, (2007)
- [3] Christesen, S., (private communication, 2005).
- [4] Kalasinsky, K., (private communication, 2004)
- [5] Schweitzer, R., Windig, W. and Treado, P.J., "Method for Identifying Components of a Mixture Via Spectral Analysis", U.S. Patent 7,072,770, (2006)